Feshbach-Einstein Condensates

V. G. Rousseau and P. J. H. Denteneer

Instituut-Lorentz, LION, Universiteit Leiden, Postbus 9504, 2300 RA Leiden, The Netherlands

(Received 21 October 2008; revised manuscript received 13 November 2008; published 6 January 2009)

We investigate the phase diagram of a two-species Bose-Hubbard model describing atoms and molecules on a lattice, interacting via a Feshbach resonance. We identify a region where the system exhibits an exotic super-Mott phase and regions with phases characterized by atomic and/or molecular condensates. Our approach is based on a recently developed exact quantum Monte Carlo algorithm: the stochastic Green function algorithm with tunable directionality. We confirm some of the results predicted by mean-field studies, but we also find disagreement with these studies. In particular, we find a phase with an atomic but no molecular condensate, which is missing in all mean-field phase diagrams.

DOI: 10.1103/PhysRevLett.102.015301 PACS numbers: 67.85.−d, 02.70.Uu, 03.75.Lm, 05.30.Jp

More than 80 years ago, Einstein predicted a remarkable phenomenon to occur in a gas of identical atoms interacting weakly at low temperature and high density [1]. Under such conditions, when the de Broglie wavelength of the atoms becomes larger than the interatomic distance, a macroscopic fraction of the atoms accumulates in the lowest energy state. This phenomenon, known as Bose-Einstein condensation, remained in the archives for a long time, and was reconsidered later with the discovery of the superfluidity of Helium in 1937. It is only in 1995 with the advent of laser cooling techniques that the first Bose-Einstein condensates of atoms were achieved [2,3]. At present, experiments trying to achieve ultracold and degenerate molecular gases are creating considerable excitement [4–6]. These experiments should lead to the creation of long-lived molecular Feshbach-Einstein condensates, with applications in the fields of precision measurements and quantum information [7].

Near a Feshbach resonance, molecules are formed from atoms by tuning a magnetic field and bringing into resonance scattering states of atoms with molecular bound states [8]. In this way, conversions between atoms and diatomic molecules are induced. A model Hamiltonian that describes mixtures of atoms and molecules was introduced and studied before [9–12]. In this Letter, we study this model and analyze the presence or not of atomic and/or molecular condensates, using the recently developed stochastic Green function (SGF) algorithm [13] with tunable directionality [14]. With this exact quantum Monte Carlo (QMC) algorithm, momentum distribution functions, which are the main indicators of condensation, are easily accessible and allow direct comparisons with experiments. We critically compare our results with the predictions of mean-field (MF) studies [10,11].

We consider the model for bosonic atoms and molecules on a lattice. The particles can hop onto neighboring sites, and their interactions are described by intraspecies and interspecies onsite potentials. An additional conversion term allows two atoms to turn into a molecule, and vice versa. This leads us to consider the Hamiltonian $\hat{\mathcal{H}} = \hat{T} + \hat{P} + \hat{C}$ with

$$\hat{T} = -t_a \sum_{\langle i,j \rangle} (a_i^\dagger a_j + \text{H.c.}) - t_m \sum_{\langle i,j \rangle} (m_i^\dagger m_j + \text{H.c.}), \quad (1)$$

$$\hat{P} = U_{aa} \sum_i \hat{n}_i^a (\hat{n}_i^a - 1) + U_{mm} \sum_i \hat{n}_i^m (\hat{n}_i^m - 1) + U_{am} \sum_i \hat{n}_i^a \hat{n}_i^m + D \sum_i \hat{n}_i^m, \quad (2)$$

$$\hat{C} = g \sum_i (m_i^\dagger a_i a_i + a_i^\dagger a_i^\dagger m_i). \quad (3)$$

The $\hat{T}$, $\hat{P}$, and $\hat{C}$ operators correspond, respectively, to the kinetic, potential, and conversion energies. The $a_i^\dagger$ and a_i operators ($m_i^\dagger$ and m_i) are the creation and annihilation operators of atoms (molecules) on site i, and $\hat{n}_i^a = a_i^\dagger a_i$ ($\hat{n}_i^m = m_i^\dagger m_i$) counts the number of atoms (molecules) on site i. Those operators satisfy the usual bosonic commutation rules. The sums $\langle i, j \rangle$ run over pairs of nearest-neighbor sites i and j. We restrict our study to one dimension (1D), and we choose the atomic hopping parameter $t_a = 1$ in order to set the energy scale, and the molecular hopping parameter $t_m = 1/2$ [12]. The parameter D corresponds to the so-called detuning in Feshbach resonance physics. In this Letter, we will systematically use the same value U for the on site repulsion parameters and the conversion parameter, $U = U_{aa} = U_{mm} = U_{am} = g$, in order to simplify our study. It is important to note that the Hamiltonian does not conserve the number of atoms $N_a = \sum_i a_i^\dagger a_i$, nor the number of molecules $N_m = \sum_i m_i^\dagger m_i$ because of the conversion term (3). However, we can define the total number of particles, $N = N_a + 2N_m$, which is conserved.

While our Hamiltonian is highly nontrivial, it has become possible to simulate it exactly by making use of the SGF algorithm [13]. In this algorithm, a Green operator is considered,

$$\hat{\mathcal{G}} = \sum_{p=0}^{+\infty}\sum_{q=0}^{+\infty} g_{pq} \sum_{\{i_p|j_q\}} \prod_{k=1}^{p} \hat{\mathcal{A}}^{\dagger}_{i_k} \prod_{l=1}^{q} \hat{\mathcal{A}}_{j_l}, \tag{4}$$

where g_{pq} is an optimization matrix, $\hat{\mathcal{A}}^{\dagger}$ and $\hat{\mathcal{A}}$ are normalized creation and annihilation operators, defined as the operators that create and destroy particles without changing the norm of the state they are applied to, and $\{i_p|j_q\}$ represents two subsets of site indices in which all i_p are different from all j_p. The Green operator is used to sample an extended partition function,

$$Z(\beta, \tau) = \mathrm{Tr} e^{-(\beta-\tau)\hat{\mathcal{H}}} \hat{\mathcal{G}} e^{-\tau\hat{\mathcal{H}}}, \tag{5}$$

by propagating across the operator string obtained by expanding the exponentials of expression (5) in the interaction picture. When configurations in which $\hat{\mathcal{G}}$ acts as an identity operator occur, then (5) reduces to the partition function $Z(\beta) = \mathrm{Tr} e^{-\beta\hat{\mathcal{H}}}$, and measurements of physical quantities can be performed. In addition, the directionality of the propagation of the Green operator is tunable [14], which improves considerably the efficiency of the algorithm.

An important property of the SGF algorithm is that it works in the canonical ensemble, the canonical constraint being imposed on the total number of particles N. This is essential for the efficiency of the simulations. Indeed, our model describes a mixture of two different species of particles, and would require two different chemical potentials for a description in the grand-canonical ensemble. Adjusting numerically two chemical potentials is cumbersome because the number of particles of each species depends on all parameters of the Hamiltonian. Working in the canonical ensemble allows to set the total number of particles, and the ratio between the number of atoms and molecules is controlled via the detuning, mimicking what is done in experiments.

In order to characterize the different phases encountered, it is useful to consider the superfluid density ρ_s. The SGF algorithm samples the winding number W, so the superfluid density is simply given by $\rho_s = \langle W^2 \rangle L/2\beta$. It turns out to be more efficient to measure ρ_s by using an improved estimator W_{ext} [13] for the winding number,

$$W^2_{\mathrm{ext}} = \frac{2|\tilde{j}(\omega_1)|^2 - |\tilde{j}(\omega_2)|^2}{L^2}, \qquad \omega_1 = \frac{2\pi}{\beta}, \qquad \omega_2 = \frac{4\pi}{\beta}, \tag{6}$$

with

$$\tilde{j}(\omega) = \sum_{k=1}^{n} \mathcal{D}(\tau_k) e^{-i\omega\tau_k}, \tag{7}$$

where τ_k are the imaginary time indices of the interactions appearing when expanding the partition function (5), and $\mathcal{D}(\tau_k)$ equals 1 (-1) if a particle jumps to the right (left) at imaginary time τ_k. This improved estimator converges faster to the zero temperature value of the winding number [13]. In our case, we evaluate the atomic and molecular winding numbers, W_a and W_m, and the corresponding superfluid densities are given by $\rho_s^a = \langle W_a^2 \rangle L/2\beta$ and $\rho_s^m = \langle W_m^2 \rangle L/2\beta$. In addition, it is useful to define the correlated superfluid density ρ_s^{cor} [12],

$$\rho_s^{\mathrm{cor}} = \frac{\langle (W_a + 2W_m)^2 \rangle L}{2\beta}. \tag{8}$$

These quantities allow us to identify superfluid (SF) and super-Mott (SM) [12] phases. SF phases are characterized by nonzero values for ρ_s^a, ρ_s^m, and ρ_s^{cor}, while a vanishing value for ρ_s^{cor} with nonzero values for ρ_s^a and ρ_s^m is the signature of a SM phase (see caption of Fig. 1). The SGF algorithm allows to measure the atomic and molecular Green functions $\langle a_i^{\dagger} a_j \rangle$ and $\langle m_i^{\dagger} m_j \rangle$, from which the associated momentum distribution functions $n_a(k)$ and $n_m(k)$ are computed by performing a Fourier transformation:

$$n_a(k) = \frac{1}{L} \sum_{pq} \langle a_p^{\dagger} a_q \rangle e^{-ik(p-q)} \tag{9}$$

$$n_m(k) = \frac{1}{L} \sum_{pq} \langle m_p^{\dagger} m_q \rangle e^{-ik(p-q)}. \tag{10}$$

Because we are considering 1D systems, we can expect at most quasicondensates. These are characterized by a diverging occupation of the zero-momentum state $n(k = 0)$ as a function of the size L of the system, while the condensate fraction $n(0)/N$ vanishes in the thermodynamic limit. As a result, knowing the value of the condensate fraction for an arbitrary large system size is not sufficient to determine if the system is quasicondensed or not. One needs to perform a finite-size scaling analysis in order to determine if $n(0)$ diverges or not. In the following, all denoted "condensate" phases are to be understood as "quasicondensate" phases. As a result, the quantities $n_a(k)$ and $n_m(k)$ allow us to identify phases with atomic condensate (AC), molecular condensate (MC), or atomic + molecular condensates (AC + MC). It is also

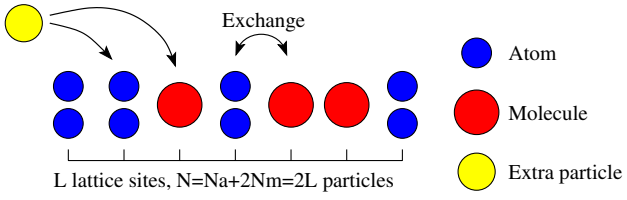

FIG. 1 (color online). Typical configuration in a SM phase. The addition of an extra particle (atom or molecule) has a finite energy cost because it creates either a triplet of atoms, or an atom-atom-molecule triplet, or a pair of molecules, or an atom-molecule pair. Thus, the phase is incompressible. However, exchanging a pair of atoms with a molecule is free, thus allowing anticorrelated supercurrents.

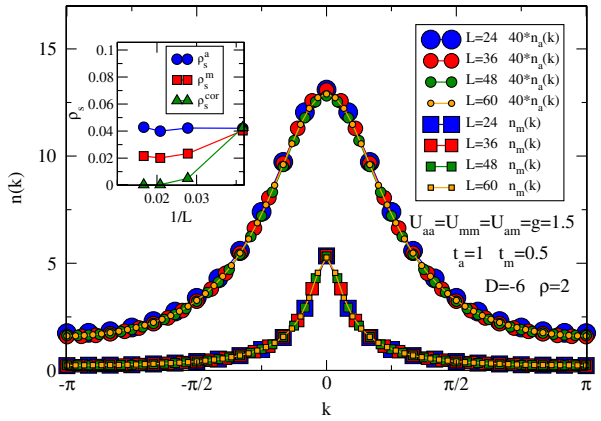

FIG. 2 (color online). Identification of the SM phase. No divergence of $n_a(0)$ or $n_m(0)$ is perceptible. The error bars are smaller than the $L = 60$ symbol size.

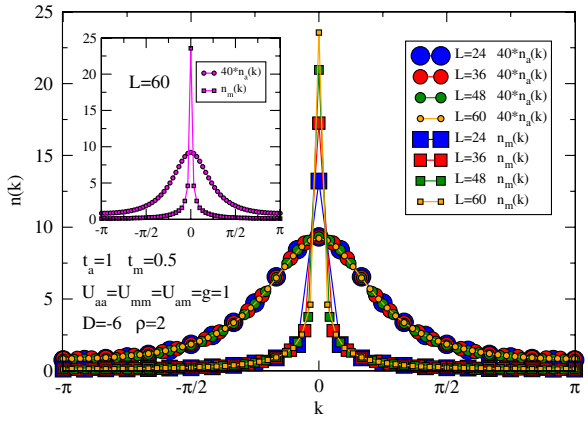

FIG. 3 (color online). Identification of the MC phase. The occupation of the zero-momentum state of molecules diverges as the size L of the system increases. The error bars are smaller than the $L = 60$ symbol size, except in $k = 0$ for molecules for which the error is about 2 times the size of the symbol.

useful to keep in mind that the areas below the curves $n_a(k)$ and $n_m(k)$ are exactly equal to N_a and N_m, respectively, thus allowing an evaluation of the population of atoms and molecules.

We concentrate our study on systems with a total density $\rho_{\text{tot}} = N/L = 2$, which is one of the cases considered in MF [11] and QMC [12] studies. We investigate the phase diagram in the $(1/U, D)$ plane. For sufficiently large interactions U, depending on the detuning D, we find an insulating phase characterized by a vanishing compressibility and the absence of global superflow. This is in agreement with MF studies. However, Ref. [11] denotes this insulating phase as a regular Mott insulator (MI), whereas we find that it is actually a more exotic SM phase (see above). This can be seen in Fig. 2 for the case $U = 1.5$ and $D = -6$. The momentum distribution functions for atoms and molecules are plotted for different sizes of the lattice. No divergence of the occupation of the zero-momentum state is perceptible, so there is neither an atomic nor a molecular condensate. Moreover, the inset shows that the correlated superfluid density ρ_s^{cor} vanishes as the system size increases, as expected for an insulating phase. However, we can see that the superfluid densities associated with the individual atomic and molecular species converge to a finite value, which is the signature of a SM phase (a similar phase is also present in the case of Bose-Fermi mixtures [15]). This is the first qualitative difference between MF results and ours.

Starting from the above SM phase, reducing the interactions will eventually break the solid structure. For $U = 1$ and negative detuning $D = -6$, the system undergoes a molecular condensation, as can be seen in Fig. 3. No divergence of the occupation of the zero-momentum state $n_a(0)$ occurs. However, $n_m(0)$ diverges and shows the presence of a molecular condensate. This transition from an insulator to a MC phase is in agreement with MF theory.

The SM phase persists when going from negative to positive detuning with large interactions. For sufficiently large detuning D, MF studies predict a direct transition from a MI (actually SM) phase to an AC + MC phase, as the interactions are reduced. However, our remarkable result is that we find an intermediate AC phase in a small region of the phase diagram. This can be seen in Fig. 4 for the case $U = 5$ and $D = 4$. We can see that a divergence of $n_a(0)$ occurs while $n_m(0)$ remains constant as the system size increases. Thus, we are in the presence of a phase in which the atoms are condensed, but not the molecules. Such an AC phase is missing, to our knowledge, in all phase diagrams coming from MF theory [10,11]. Our evidence for the AC phase in Fig. 4 is comparable to that for the MC phase in Fig. 3.

While it is hard to give a phase diagram with precise borders delimiting the different phases (because each point of the diagram requires a heavy finite-size scaling analy-

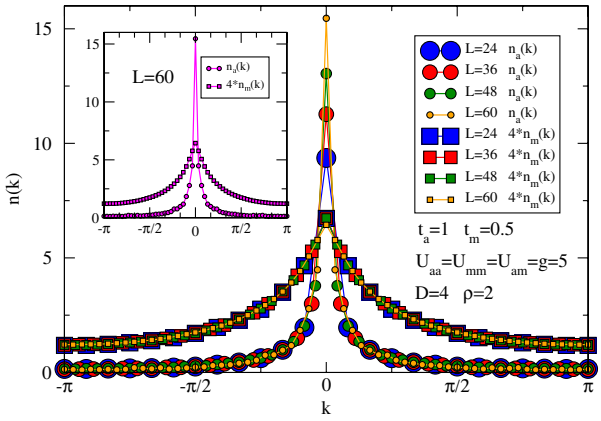

FIG. 4 (color online). Identification of the AC phase. The occupation of the zero-momentum state of atoms diverges as the size L of the system increases. The error bars are smaller than the $L = 60$ symbol size, except in $k = 0$ for atoms for which the error is about 4 times the size of the symbol.

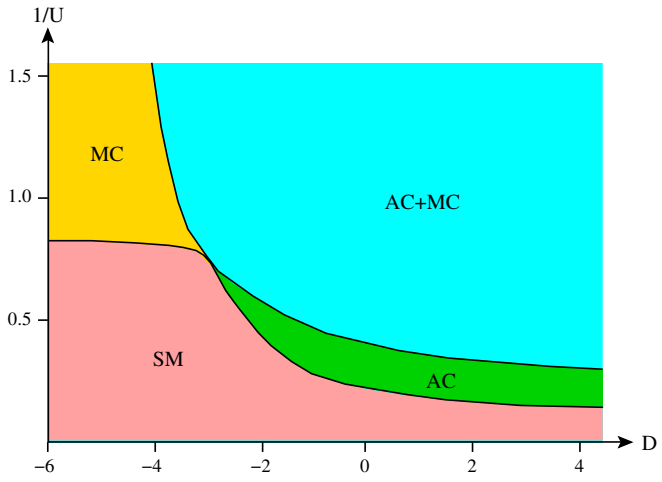

FIG. 5 (color online). The qualitative phase diagram in the $(1/U, D)$ plane for $\rho_{\mathrm{tot}} = 2$. We identify regions with super-Mott (SM), atomic condensate (AC), molecular condensate (MC), and atomic + molecular condensate (AC + MC) phases.

sis), we give a qualitative diagram in Fig. 5 based on simulations for considerably more values of the detuning D and the interaction U than in Fig. 2–4. In addition, we provide connection with future experiments by showing on Fig. 6 how the atomic and molecular visibilities $\mathcal{V}_a$ and $\mathcal{V}_m$ [16] behave when entering the AC phase from the SM phase along the vertical line $D = -2$. In the present case, $\mathcal{V}_a$ reaches unity before $\mathcal{V}_m$ as the interactions decrease, showing again that the system is entering an AC phase.

To conclude, we have studied a two-species Bose-Hubbard Hamiltonian for atoms and molecules on a lattice, interacting via a Feshbach resonance. We have shown that

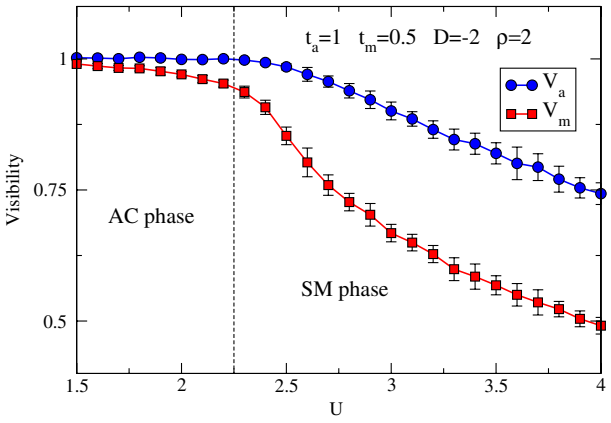

FIG. 6 (color online). The atomic and molecular visibilities $\mathcal{V}_a$ and $\mathcal{V}_m$. Because of the divergence of $n_a(0)$ or $n_m(0)$, $\mathcal{V}_a$ (and/or $\mathcal{V}_m$) must converge to unity when an atomic (and/or a molecular) condensate occurs.

the MI phase identified in MF studies is actually a SM phase. For large negative detuning, we find a transition from this insulating phase to a MC phase, in agreement with MF theory. For smaller negative or positive detuning, however, while MF theory predicts a direct transition from MI to AC + MC, we find that an AC phase occurs and that the system undergoes phase transitions from SM to AC to AC + MC. The AC phase was not found in previous studies. The phase diagram we provide may serve as a guide for the investigation of atomic and molecular quantum matter now that condensation of Feshbach molecules is beginning to be achieved experimentally.

We would like to thank Frédéric Hébert for useful conversations. This work is part of the research program of the "Stichting voor Fundamenteel Onderzoek der Materie (FOM)," which is financially supported by the "Nederlandse Organisatie voor Wetenschappelijk Onderzoek (NWO)."

[1] A. Einstein, *Quantentheorie DES einatomigen idealen Gase, Zweite Abhandlung* (Sitzungsberichte der Preussischen Akademie der Wissenschaften, Berlin, Physikalisch-mathematische Klasse, 1925).
[2] E. A. Cornell, C. E. Wieman *et al.*, Science **269**, 198 (1995).
[3] W. Ketterle *et al.*, Phys. Rev. Lett. **75**, 3969 (1995).
[4] F. Lang, K. Winkler, C. Strauss, R. Grimm, and J. H. Denschlag, Phys. Rev. Lett. **101**, 133005 (2008).
[5] J. Deiglmayr, A. Grochola, M. Repp, K. Mörtlbauer, C. Glück, J. Lange, O. Dulieu, R. Wester, and M. Weidemüller, Phys. Rev. Lett. **101**, 133004 (2008).
[6] K.-K. Ni, S. Ospelkaus, M. H. G. de Miranda, A. Pe'er, B. Neyenhuis, J. J. Zirbel, S. Kotochigova, P. S. Julienne, D. S. Jin, and J. Ye, Science **322**, 231 (2008).
[7] D. DeMille *et al.*, Phys. Rev. Lett. **100**, 043202 (2008).
[8] T. Köhler, K. Góral, and P. S. Julienne, Rev. Mod. Phys. **78**, 1311 (2006).
[9] E. Timmermans, P. Tommasini, M. Hussein, and A. Kerman, Phys. Rep. **315**, 199 (1999).
[10] D. B. M. Dickerscheid, U. Al Khawaja, D. van Oosten, and H. T. C. Stoof, Phys. Rev. A **71**, 043604 (2005).
[11] K. Sengupta and N. Dupuis, Europhys. Lett. **70**, 586 (2005).
[12] V. G. Rousseau and P. J. H. Denteneer, Phys. Rev. A **77**, 013609 (2008).
[13] V. G. Rousseau, Phys. Rev. E **77**, 056705 (2008).
[14] V. G. Rousseau, Phys. Rev. E **78**, 056707 (2008).
[15] A. Zujev, A. Baldwin, R. T. Scalettar, V. G. Rousseau, P. J. H. Denteneer, and M. Rigol, Phys. Rev. A **78**, 033619 (2008).
[16] F. Gerbier, A. Widera, S. Fölling, O. Mandel, T. Gericke, and I. Bloch Phys. Rev. Lett. **95**, 050404 (2005).